

See discussions, stats, and author profiles for this publication at: <https://www.researchgate.net/publication/258999105>

Scalable open- and balance-type calorimeter for measuring power electronics and motors

Conference Paper · November 2013

DOI: 10.1109/IECON.2013.6699623

CITATIONS

5

READS

65

6 authors, including:



Antti Kosonen

Lappeenranta – Lahti University of Technology LUT

76 PUBLICATIONS 507 CITATIONS

[SEE PROFILE](#)



L. Aarniovuori

Lappeenranta – Lahti University of Technology LUT

50 PUBLICATIONS 287 CITATIONS

[SEE PROFILE](#)



J. Pyrhönen

Lappeenranta – Lahti University of Technology LUT

437 PUBLICATIONS 5,306 CITATIONS

[SEE PROFILE](#)



Jero Ahola

Lappeenranta – Lahti University of Technology LUT

150 PUBLICATIONS 964 CITATIONS

[SEE PROFILE](#)

Some of the authors of this publication are also working on these related projects:



Controller for Bridge Configured Winding based Bearing-less Motor [View project](#)



ODES aCSESS: Optimal design and control of cruise ship energy systems [View project](#)

Scalable Open- and Balance-Type Calorimeter for Measuring Power Electronics and Motors

Antti Kosonen, Lassi Aarniovuori, Juha Pyrhönen,
Jero Ahola, and Markku Niemelä
Department of Electrical Engineering
Lappeenranta University of Technology
P.O. Box 20, FI-53851 Lappeenranta, Finland
antti.kosonen@lut.fi

Kari Tammi
VTT
P.O. Box 1000, FI-02044 VTT, Finland
kari.tammi@vtt.fi

Abstract—Accurate measurement of losses of high-efficiency power electronics devices and electrical motors is difficult by using input and output powers. In the calorimetric method, these losses are measured directly. However, the calorimeters have to be designed for a certain power loss range, and therefore, the same system cannot be applied to different power devices. In this paper, a functional and scalable power loss measurement concept is suggested for the measurement of losses between 10 W and 30 kW with a reasonable measurement accuracy. Such a power loss range can be applied, for example, to devices with 97% efficiencies with input powers between 333 W and 1 MW. The concept is introduced, verified, and demonstrated by laboratory measurements.

Keywords—Calorimetry; converters; electric machines; energy efficiency; loss measurement; motors; power electronics; solar power generation

I. INTRODUCTION

High-efficiency equipment makes the efficiency determination with the traditional input-output method an even more challenging task. Hence, the calorimetric method is an attractive alternative for loss measurements. However, the measurement of different power losses and devices of varying sizes require different calorimeters.

An overview of various loss measurement techniques for power electronics systems is given, the electrical methods are introduced, and sources of measurement errors are discussed in [1]. Calorimetric systems are divided into four categories: open, close, balance, and series types in [2].

Different kinds of calorimeters are constructed to obtain losses of electrical devices. These calorimeters can be divided in two basic types, open type with air as a coolant [3]–[8] and close type with water as a coolant [9]–[13]. The systems introduced in [3]–[5] are open- and balance-type calorimeters. The specific version of an open- and balance-type calorimeter, the series calorimeter, uses two successive chambers, and the balance test is performed simultaneously in another chamber with a reference heater [6]. Another case is that these two chambers are in parallel [7]. The system used in [8] can be termed direct calorimeters that are based on the measurement and calculation of air properties. These systems neglect the time-consuming balance test.

The components of a calorimeter, such as a blower, the size of a chamber, tubes, etc., can be scaled to different sizes but some requirements should be taken into account in the design phase. This paper introduces a calorimeter concept that can be scaled to different power loss levels. The scaling procedure is carried out for the measurement range of power losses between 10 W and 30 kW. The previous calorimetric systems proposed in the literature for the same purposes are often complex, specially tailored systems, and they are not easily scaled to different ranges.

This paper is organized as follows. Section II introduces the basic concept and its properties. Section III describes the designed and built calorimeters. Verification tests are carried out in Section IV. Design and measurement aspects are discussed in Section V. Section VI concludes the paper.

II. SCALABLE CALORIMETRIC CONCEPT

The concept introduced in this paper is intended and designed for measuring the power losses of power electronics and electric motors from 10 W up to 30 kW within uncertainties of 0.3%–0.7%.

The open- and balance-type calorimeter was chosen for this concept, because the balance test minimizes the number of measurements that have a direct effect on the uncertainty of the whole system. The basic idea of the balance-type calorimeter is to define the power losses of a device or a system indirectly with the balance test by using a reference heater, the power of which can be measured accurately. The heater and the device to be tested are assumed to have similar heat emission characteristics, and the main heat flux is emitted to the air flowing through the calorimeter. The basic concept of calorimetric measurements is illustrated in Fig. 1.

A. Structure

The basic construction is a single box with polyurethane as the insulation material to minimize uncontrolled heat fluxes. The chamber is designed according to the size of the devices to be measured. In addition to DUT (device under test), there has to be space reserved for a heater.

B. Instrumentation

The instrumentation includes devices that are connected to the computer for control purposes or for further study. A-class

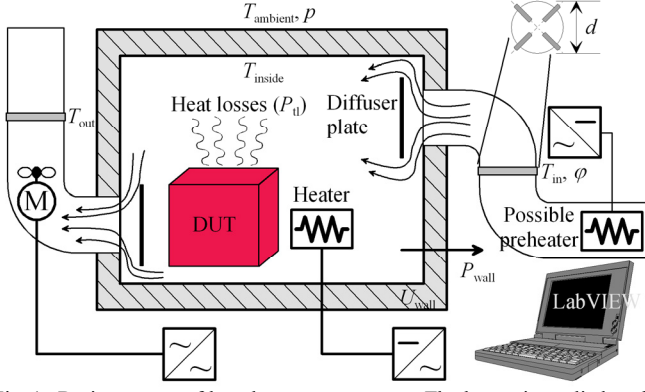


Fig. 1. Basic concept of heat loss measurements. The heater is applied to the balance test and to warm the chamber before start. The temperature sensors at the inlet and outlet tubes are at a 90° angle to each other, and the distance from another sensor is $d/3$.

PT-100 temperature sensors with four-wire compensation circuits are applied to measure the inlet, outlet, and inside temperatures. The temperature sensors are read by a Keithley 2701 data acquisition system with a Keithley 7702 40-channel differential multiplexer module. In addition, ambient air humidity and barometric pressure in the laboratory are measured.

The inlet and outlet temperatures (T_{in} and T_{out}) are averaged from four sensors (see the cross-section in Fig. 1). These sensors are at a 90° angle to each other, and the distance between adjacent sensors is $d/3$. Therefore, the length of these sensors depends directly on the diameter of the tube. Temperatures are measured after mixing the air (a blower in the outlet) to equalize the temperature inside the tube before the temperature sensors. In addition, in the temperature measurement locations the air is circulating from down to up as illustrated in Fig. 1 to reduce the separation of air into layers because of natural convection.

Inside the chamber, temperature sensors are located close to the corners and in the middle of the walls. The number of sensors is the larger the more voluminous the chamber is. There are diffuser plates in the front of the inlet and outlet tubes to remove direct heat radiation to the tubes. This removes the effect of the heat source locations in the chamber on that proportion of the heat power that is transferred by the air flow. Therefore, the location of the heat source affects only that proportion of the losses that result from the heat leakage through the walls. The heat losses calculated from the temperature difference (T_{inside} and $T_{ambient}$) and overall heat transfer coefficient through the calorimeter walls and wall joints are assumed to be independent of the device to be tested.

The blower exhausts to the atmosphere and produces a slight vacuum inside the chamber. The volume flow of the exhaust blower is set to remove the maximum designed heat power from the chamber with a temperature difference of 20 K between T_{out} and T_{in} that are averaged from four sensor values. The exhaust blower is controlled by a PID speed controller, in which the output temperature is used as the reference value for the control. For this purpose, a radial blower equipped with a rotational speed meter supplied by a frequency converter is recommended. The diameters of the tubes are selected

according to the suction-side cross-sectional area of the exhaust blower.

For the balance test, a resistor is applied as a heater. The heater is also used when the chamber and the DUT are heated before the measurements. This way, the thermal equilibrium state can be reached faster than starting the measurement with a cold chamber. The DUT rated surface temperature is usually known a priori, at least to a certain degree, and it is advisable to heat the chamber at least to this known temperature before commencing the actual test. The resistor is driven by a DC power supply. The heater should be selected according to the voltage and current ranges of the DC power supply. The DC power is measured by a power analyzer with a power accuracy of 0.1% of reading + 0.1% of range used in the measurement. The DC power measurement uncertainty has a direct impact on the whole system measurement uncertainty. An air preheater driven by a DC power supply can be used to keep the inlet air at a constant temperature. A PI controller with the inlet air temperature feedback is controlling the preheater power.

III. DESIGNED CALORIMETERS

The power loss range is divided into three parts, because the blowers are known to operate properly in the range of about 1:10 of the nominal flow rate/pressure. In addition, the size of the chambers should be reasonable for the devices to be measured.

A. Small-Size Calorimeter

The chamber of the small-size calorimeter is designed to measure power losses up to 300 W. The chamber has internal dimensions of $0.3 \text{ m} \times 0.3 \text{ m} \times 0.3 \text{ m}$ ($l \times w \times h$). A sandwich form of a 100 mm polyurethane insulation between two layers of fiberglass laminates is employed in the structure. The inside temperature distribution of the chamber T_{inside} is measured from a grid of four sensors in the middle of each inner wall and the ambient temperature distribution of the chamber $T_{ambient}$ from a single sensor. Two wire-wound flat resistors in aluminum enclosures are applied as heaters. Both of them withstand 150 W of continuous DC power, and are located in both sides of the walls.

The exhaust blower is placed at the top of the chamber to prevent the formation of a heat storage by natural convection to the chamber roof in the case of low flow rates. The maximum designed volume flow rate of the blower is scaled to $45 \text{ m}^3/\text{h}$. For this purpose, we did not find a commercial blower that can be driven by a frequency converter. Therefore, a centrifugal DC blower of 14 W with the nominal rotational speed of 2850 rpm was modified for this purpose, because plain impellers were not available. The DC motor was removed and a three-phase 90 W induction motor with the nominal rotational speed of 2820 rpm was selected instead. The motor is equipped with a rotational speed meter, and it can be driven by a frequency converter. The diameter of the inlet and outlet tubes is 50 mm. Fig. 2(a) illustrates the experimental setup of the calorimeter.

B. Medium-Size Calorimeter

The chamber of the medium-size calorimeter is designed to measure power losses up to 2 kW. The chamber has internal

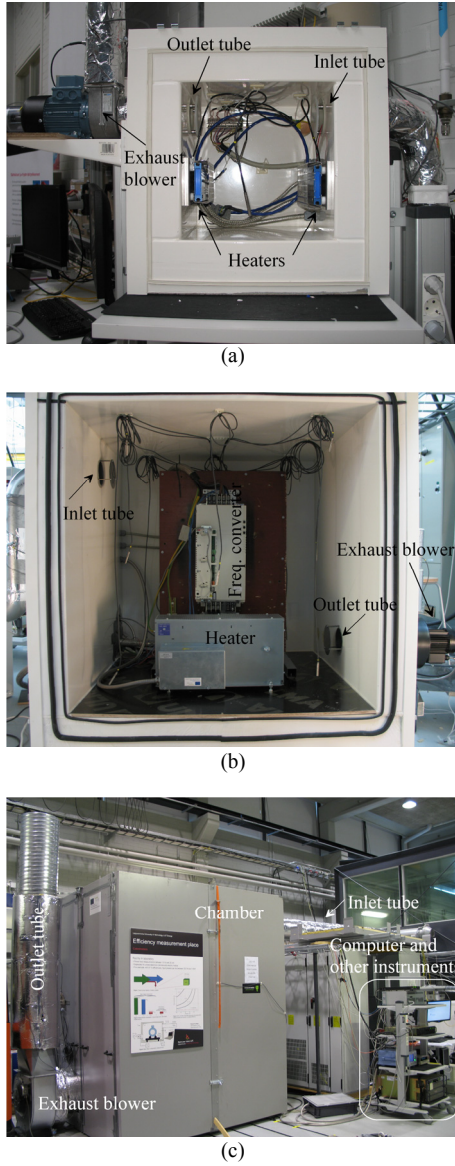


Fig. 2. Experimental calorimeter setup. (a) Small size. (b) Medium size. (c) Large size.

dimensions of $1\text{ m} \times 1\text{ m} \times 1\text{ m}$ ($l \times w \times h$). A sandwich form of a 120 mm polyurethane insulation between two layers of fiberglass laminates is employed in the structure. The inside temperature distribution of the chamber T_{inside} is measured from a grid of 12 sensors (eight sensors altogether located in each corner and four sensors in the middle of each inner wall) and the ambient temperature distribution of the chamber T_{ambient} from a single sensor. A basic steel-grid-fixed resistor is applied as a heater that withstands 2 kW of continuous DC power.

In this case, the exhaust blower is placed at the bottom of the chamber. The inlet tube is located at the top of the chamber so that the air is circulating from up to down. The maximum designed volume flow rate is scaled to $300\text{ m}^3/\text{h}$. For this purpose, a radial blower that can be supplied by a frequency converter is selected. The blower is a three-phase and 180 W one with a nominal rotational speed of 2730 rpm. The blower is equipped with a rotational speed meter. The diameter of the

inlet and outlet tubes is 100 mm. Fig. 2(b) illustrates the experimental setup of the calorimeter.

C. Large-Size Calorimeter

The chamber of the large-size calorimeter is designed to measure power losses up to 30 kW. The chamber has internal dimensions of $2\text{ m} \times 2\text{ m} \times 2.5\text{ m}$ ($l \times w \times h$). A sandwich form of 100 mm polyurethane insulation between two layers of steel plates is employed in the structure. The inside temperature distribution of the chamber T_{inside} is measured from a grid of 16 sensors (eight sensors altogether located in each corner, four sensors in the midpoint of the floor and roof corners, and four sensors in the middle of each inner wall) and the ambient temperature distribution of the chamber T_{ambient} from four sensors (one in each wall). A basic steel-grid-fixed resistor is applied as a heater that withstands 30 kW of continuous DC power.

The exhaust blower is placed at the bottom of the chamber. The inlet tube is located at the top of the chamber so that air is circulating from up to down. The maximum designed volume flow rate of the blower is scaled to $4500\text{ m}^3/\text{h}$. For this purpose, a radial blower that can be supplied by a frequency converter is selected. The blower is a three-phase and 2.7 kW one with a nominal rotational speed of 830 rpm. The blower is equipped with a rotational speed meter. The diameter of the inlet and outlet tubes is 400 mm. Fig. 2(c) illustrates the experimental setup of the calorimeter.

IV. LABORATORY MEASUREMENTS

The uncertainties of all the calorimeters were verified. The verification results for the medium-size calorimeter are presented in [14] and for the large-size calorimeter in [15]. The combined uncertainties of the small-, medium-, and large-size calorimeters are 0.3%, 0.4%, and 0.7%, respectively. The combined uncertainty includes the uncertainty of the calorimeter and the DC power measurement. The verification results are illustrated in Fig. 3. In the verification tests, the balance test heater was used to emulate the measured heat source. In addition, the verification tests with the medium-size calorimeter include a specifically constructed heat source. The purpose of this is to study whether the heat source shape, place, or extra ventilation of the device has an impact on the results.

The measurement procedure is presented in detail in [16]. The procedure includes calibration, in which the main objective is to define the estimated mass flow rate as a function of blower rotational speed. The calibration is carried out only at the beginning of the measurement series. Calibration curves are illustrated in Fig. 4.

For the motor drive loss measurement, two medium-size chambers were constructed, one for frequency converters and another for motors. Now, both of these can be measured simultaneously. The results of one calorimetric measurement series of 37 kW electric drives are given in [17]. Although having equal rated powers, the thermal time constants and powers of the cooling blowers of the frequency converter and the motor are totally different from each other. The cooling blower power of 37 kW frequency converters varies from 15 W to 40 W, while the blower of the TEFC motor with the same rating is typically from 100 W to 200 W. The most common

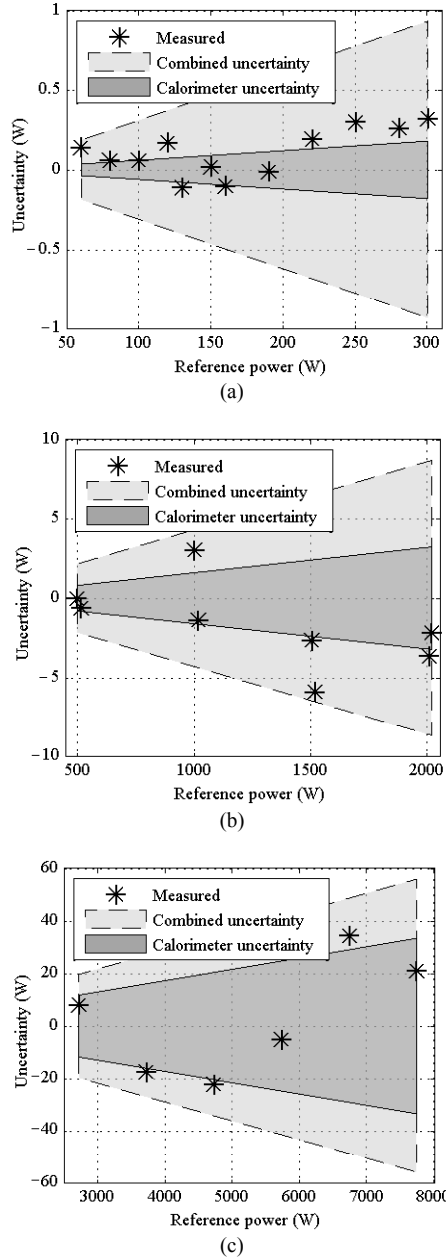


Fig. 3. Calorimeter verification test. Combined uncertainty includes the uncertainty of the calorimeter and the DC power measurement. (a) Small size. (b) Medium size. (c) Large size.

cooling design in the frequency converter frame is to place the ventilation blower at the top of the frame so that it sucks the air through the frame. Thus, the device ventilation blower circulates the air in vertical direction. In the TEFC motor, the blower is placed at the end of the motor shaft in the non-drive end, and the blower circulates the air in the axial direction. One concern in the motor calorimetric measurement was that the motor blower may disturb the air flow produced by the chamber exhaust blower.

A. Frequency Converter Losses in Medium-Size Calorimeter

The frequency converter losses were measured using a Yokogawa WT1600 power analyzer with a HITEC Zero-Flux™ current (300 A maximum peak current) measurement system

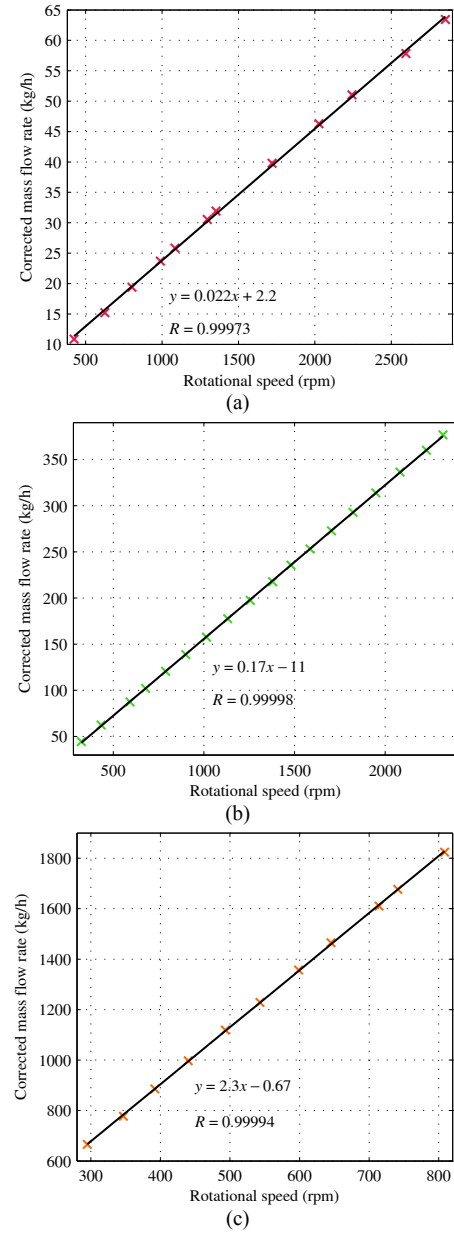


Fig. 4. Calibration curves for the corrected mass flow rate as a function of the rotational speed of the blower. The points are corrected to the reference conditions ($T_{in} = 22^\circ\text{C}$, $T_{out} = 40^\circ\text{C}$, $\phi = 20\%$ RH, and $p = 101325\text{ Pa}$). (a) Small size. (b) Medium size. (c) Large size.

and the calorimetric system simultaneously. The input and output voltages were sensed directly from the converter terminals, and the current sensors were mounted in the close vicinity of the calorimeter. The 34 W frequency converter ventilation blower was fed from an external DC source to keep the chamber conditions similar during the main and balance tests. Six measurement points with a squared load were used; the load comprises machines operating by centrifugal force, such as centrifuges, centrifugal pumps, and fans. The numerical results of the measurement series are given in Table I. The differences between calorimetric and electric measurements in the efficiency and losses are shown in Fig. 5. According to Fig. 5, there is a loss difference in the measurement results. The calorimetric efficiencies are calculated using the measured

TABLE I. FREQUENCY CONVERTER MEASUREMENT RESULTS

Meas. point	1	2	3	4	5	6
f_{out} (Hz)	10	25	40	45	50	62.5
T_{motor} (%)	13	23	59	75	92	73.6
$U_{in,RMS}$ (V)	232.3	230.6	231.2	232.7	232.2	230.3
$I_{in,RMS}$ (A)	3.9	10.7	32.6	44.4	58.2	59.0
$I_{out,RMS}$ (A)	26.7	29.6	46.5	55.2	67.7	67.5
P_{in} (W)	1591	5216	19615	27615	37418	37554
P_{out} (W)	1315	4881	19088	26987	36680	36811
$P_{tl,io}$ (W)	310	369	561	662	772	777
$P_{tl,cal}$ (W)	320	378	571	668	789	800
ΔP (W)	+10	+9	+10	+6	+17	+23

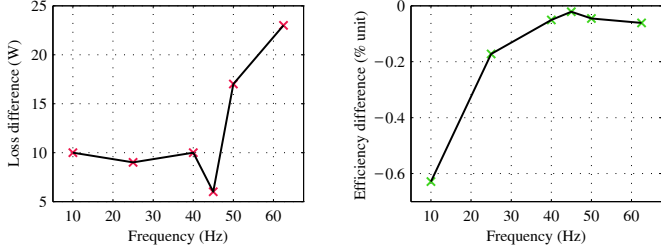


Fig. 5. Efficiency and loss difference between the calorimetric and electric measurements in the frequency converter measurements.

electric input power of the converter. The uncertainty in the loss determined by the electric measurement in all measurement points in this measurement series is over ± 100 W. Thus, in this case, the calorimeter can be considered to give more reliable results than the electric measurements.

B. Motor Losses in Medium-Size Calorimeter

In the balance-type calorimeter, it is assumed that the measurement conditions remain the same during the main and balance tests. In the calorimetric measurements of the motor, the motor can be rotated with the load machine during the balance test to keep the ventilation conditions similar in both tests. This kind of a measurement procedure involves two problems: the first problem is related to the uncertainty of the calorimetric measurement. If the total losses of the motor are measured, the motor losses are determined against the known power that is the heater power during the balance test plus the friction and windage losses. Therefore, the same uncertainty that is in the friction and windage losses is associated with the total losses of the motor, but if the motor losses can be determined when the motor is not rotating, the uncertainty in the motor losses is directly related to the uncertainty of the calorimeter. The second problem is that the friction and windage losses of the motor are temperature related. Thus, when the motor bearings are not in the same temperature in the balance test as during the main test, also the friction and windage losses are different. Especially, the hot air viscous friction of the motor air gap is smaller than the cold air friction. Therefore, the motor was equipped with a separate blower, and the balance test was repeated with this blower on and off. The three-phase blower power was measured with Yokogawa PZ4000, and the result was 170 W. During the balance test, the frequency-converter-driven chamber exhaust blower is driven with a fixed speed of 1251 rpm, and thus, the blower power is directly related to the torque of the motor. The exhaust blower power is directly proportional to the amount of air that the

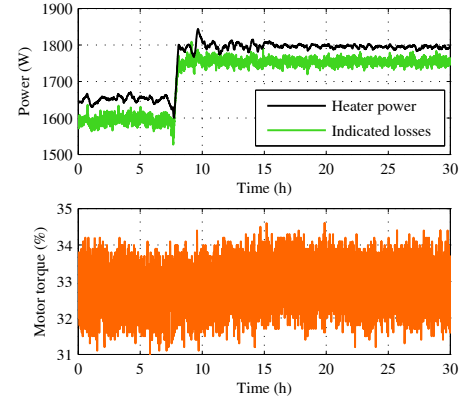


Fig. 6. Heater power, indicated losses, and motor torque of the exhaust blower during the balance test when a motor is measured in the calorimeter.

TABLE II. SOLAR CONVERTER MEASUREMENT RESULTS

Meas. point	1	2	3	4	5
P_{in} (W)	126362	126411	125711	126211	126381
P_{out} (W)	124334	124453	124420	124330	124280
$P_{tl,io}$ (W)	2028	1959	1291	1881	2101
$P_{tl,cal}$ (W)	2354	2349	2387	2426	2410
ΔP (W)	+326	+390	+1096	+545	+309

blower is removing from the chamber. The measurement curves during the balance test are shown in Fig. 6.

Fig. 6 shows that there are no rapid changes in the exhaust blower motor torque when the DUT blower is switched off. When the blower is switched off, the PI controller rapidly changes the heater power to a greater value. The indicated loss change is 171 W, which is the blower power of the motor. The results indicate that the blower power can be separated from the measured total loss of 1753 W. The results clearly show that there is no interference between the DUT blower and the chamber exhaust blower in this case. This verifies that an open-and balance-type calorimeter of this kind is well feasible for motor measurements when the chamber construction is designed so that the motor conduction losses through the motor supports and shaft cannot affect the loss measurement results.

C. Solar Power Converter Losses in Large-Size Calorimeter

The results of the European efficiency measurement [18] for a 250 kW high-efficiency grid-connected solar inverter are presented in [15]. The efficiency measurements of the converter are performed both by the electrical input-output and calorimetric methods. Further, the measurement results and their uncertainties are analyzed and discussed. To this end, the repeatability of the calorimetric results in a single operating point is tested. The efficiency value of a high-efficiency solar converter is challenging to determine accurately. The conversion efficiency of the converter is about 98.5% in this operating point, and therefore, even the slightest error in the input or output measurement can be seen in the loss results. Here, a Yokogawa WT1600 power analyzer with a HITEC Zero-Flux™ current (3000 A maximum peak current) measurement system is used. The converter was driven with a 125 kW power reference and DC input voltage reference is set to 500 VDC. The input current is 253 A, the output voltage 311 V, and the output current 233 A. The measurement results are given in Table II. The results show that the measured

output power fluctuates less than ± 100 W, but the differences in the measured input power are considerable. The difference in the measured input power between the second and third measurement point is 700 W, but at the same time, the difference in the calorimetric loss result is less than 50 W. The standard deviation in the calorimetric loss results is 30.7 W, while in the electric measurement it is 419 W (329 W if measurement point 3 is neglected).

V. DISCUSSION ON DESIGN AND MEASUREMENT ASPECTS

Various phenomena were detected in the verification, calibration, and measurement phases of the calorimeters. The significance of these phenomena depends directly on the size and dimensions of the calorimeter. In the small-size calorimeter, a heat storage causes problems to the blower control when the power losses are below 100 W because the mass flow rate is low (about 16 m³/h). The heat storage is discharged when the rotational speed of the blower is increased, and thereby, also the outlet temperature rises. The system is then driven to an unstable state, in which the heat storage is charged and then discharged over and over again. On the other hand, base power can be supplied by the heater in the main test in order to stabilize the measurement system. The practical minimum for the measurable power losses without the base power for the small-, medium-, and large-size calorimeters are 100 W, 300 W, and 2000 W, respectively. For smaller power losses, the base power is recommended. When the power losses are at the minimum level of the calorimeter, the ratio of the power losses through the walls to the losses through the air is at the highest level. The maximum level of the measurement range is restricted by the power of the heater and the exhaust blower. The largest chamber was verified up to 8 kW, because these were the largest losses in the measurement series. Temperature gradients inside the tubes are the larger the bigger is the diameter of the tube. These gradients are minimized by mixing air before the measurement and measuring the temperature when air is flowing from down to up. Without these actions, over 2 °C gradients were measured in the outlet tube of the large-size calorimeter.

VI. CONCLUSION

When the losses of a high-power system are relatively low, accurate efficiency measurements become difficult. A practical and scalable concept for calorimetric efficiency measurements of industrial converters and motors is proposed in this paper. The developed measurement concept is introduced, verified, and demonstrated by laboratory tests. The results show that the same calorimetric concept can be applied in power loss measurements of wide range. The high-efficiency device losses determined by the input-output method using a power analyzer may have a large uncertainty when distorted waveforms are analyzed.

ACKNOWLEDGMENT

This work was supported in part by the European Regional Development Fund, the City of Lappeenranta, ABB Oy, Vacon PLC, The Switch, and LUT Energy, Lappeenranta University of Technology.

REFERENCES

- [1] C. Xiao, G. Chen, and W.G.H. Odendaal, "Overview of power loss measurement techniques in power electronics systems," *IEEE Trans. Ind. Appl.*, vol. 43, no. 3, pp. 657–664, May/June 2007.
- [2] W. Cao, G.M. Asher, X. Huang, H. Zhang, I. French, J. Zhang, and M. Short, "Calorimeters and techniques used for power loss measurements in electrical machines," *IEEE Instrum. Meas. Mag.*, vol. 13, no. 6, pp. 26–33, December 2010.
- [3] B. Baholo, P.H. Mellor, D. Howe, and T.S. Birch, "An automated calorimetric method of loss measurement in electrical machines," *J. Magn. Magn. Mater.*, vol. 133, no. 1–3, pp. 433–436, May 1994.
- [4] D.R. Turner, K.J. Binns, B.N. Shamsadeen, and D.F. Warne, "Accurate measurement of induction motor losses using balance calorimeter," *IEE Electr. Power Appl.*, vol. 138, no. 5, pp. 233–242, September 1991.
- [5] A.P. Van den Bossche, D.M. Van de Sype, and V. Valchev, "Flow calorimeter for equipment test," in *Proc. 31st Annu. Conf. IEEE Industrial Electronics Society*, Raleigh, NC, USA, November 2005, pp. 860–864.
- [6] A. Jalilian, V.J. Gosbell, B.S.P. Perera, and P. Cooper, "Double chamber calorimeter (DCC): a new approach to measure induction motor harmonic losses," *IEEE Trans. Energy Convers.*, vol. 14, no. 3, pp. 680–685, September 1999.
- [7] L. Aarniovuori, A. Kosonen, M. Niemelä, and J. Pyrhönen, "Parallel chamber calorimetric concept," in *Proc. 15th European Conf. on Power Electronics and Applications*, Lille, France, September 2013, pp. 1–9.
- [8] W. Cao, K.J. Bradley, and A. Ferrah, "Development of a high-precision calorimeter for measuring power loss in electrical machines," *IEEE Trans. Instrum. Meas.*, vol. 58, no. 3, pp. 570–577, March 2009.
- [9] S. Weier, M.A. Shafi, and R. McMahon, "Precision calorimetry for the accurate measurement of losses in power electronic devices," *IEEE Trans. Ind. Appl.*, vol. 46, no. 1, pp. 278–284, January/February 2010.
- [10] P.D. Malliband, D.R.H. Carter, B.M. Gordon, and R.A. McMahon, "Design of a double-jacketed, closed type calorimeter for direct measurement of motor losses," in *Proc. 7th Int. Conf. on Power Electronics and Variable Speed Drives*, London, UK, September 1998, pp. 212–217.
- [11] P.D. Malliband, N.P. van der Duijn Schouten, and R.A. McMahon, "Precision calorimetry for the accurate measurement of inverter losses," in *Proc. 5th Int. Conf. Power Electronics and Drive Systems*, vol. 1, Singapore, November 2003, pp. 321–326.
- [12] E. Ritchie, J.K. Pedersen, F. Blaabjerg, and P. Hansen, "Calorimetric measuring systems," *IEEE Ind. Appl. Mag.*, vol. 10, no. 3, pp. 70–78, May/June 2004.
- [13] B. Szabados and A. Mihalcea, "Design and implementation of a calorimetric measurement facility for determining losses in electrical machines," *IEEE Trans. Instrum. Meas.*, vol. 51, no. 5, pp. 902–907, October 2002.
- [14] A. Kosonen, L. Aarniovuori, J. Pyrhönen, M. Niemelä, and J. Backman, "Calorimetric concept for measurement of power losses up to 2 kW in electric drives," *IET Electr. Power Appl.*, vol. 7, no. 6, pp. 453–461, July 2013.
- [15] L. Aarniovuori, A. Kosonen, P. Sillanpää, and M. Niemelä, "High-power solar inverter efficiency measurement by calorimetric and electric methods," *IEEE Trans. Power Electron.*, vol. 28, no. 6, pp. 2798–2805, June 2013.
- [16] A. Kosonen, L. Aarniovuori, J. Ahola, J. Backman, J. Pyrhönen, and M. Niemelä, "Loss definition of electric drives by a calorimetric system with data processing (Accepted for publication)," *IEEE Trans. Ind. Electron.*, early access article available.
- [17] L. Aarniovuori, A. Kosonen, M. Niemelä, and J. Pyrhönen, "Calorimetric measurement of variable-speed induction motor," in *Proc. 20th Int. Conf. on Electrical Machines*, Marseille, France, September 2012, pp. 870–876.
- [18] IEC 61683: Photovoltaic systems – power conditioners – procedure for measuring efficiency, November 1999, pp. 1–20.